Biointerface Research in Applied Chemistry
Platinum Open Access Journal (ISSN: 2069-5837)

Article
Volume 12, Issue 4, 2022, 4961 - 4973
https://doi.org/10.33263/BRIAC124.49614973

Blocking Effect of Natural Alkaloids on COVID-19 Pentameric Ion Channel: An *in silico* Perspective

Mohammad Bayati [1], Samad Nejad Ebrahimi [1,*]

[1] Department of Phytochemistry, Medicinal Plants and Drugs Research Institute, Shahid Beheshti University, Tehran, Iran
* Correspondence: s_ebrahimi@sbu.ac.ir (S.N.E.);

Scopus Author ID 9338406700

Received: 3.08.2021; Revised: 10.09.2021; Accepted: 14.09.2021; Published: 17.10.2021

Abstract: Numerous deaths worldwide have been caused by the coronavirus pandemic and are currently progressing with successive mutations and a lack of appropriate and definitive treatment. One of the drug targets to control the replication of the virus and treat this disease is to block the ion channel of the virus. This will lead to its death by disturbing the internal balance of the virus. Natural compounds such as alkaloids are usually known as effective compounds due to their medicinal characteristics and easy access to their sources. To this end, more than 3,200 natural alkaloid structures interacted with pentameric ion channels. Alkaloid compounds established significant and stable interactions with the channel. More clearly and in more detail, six alkaloid compounds with the best pharmacokinetics and binding affinity of less than -10.52 kcal/mol were selected as hit and suitable compounds for virus control. The compound of psammaplysin U (NA-1) with a binding affinity of -13.52 kcal/mol and binding free energy of -82.21 kcal/mol established hydrogen interactions with the amino acid of Val 25 in the B chain of the ion channel, which placed the compound at the top of the selected compounds. The molecular dynamics simulation of the ligand-protein complex in the 100 ps trajectory showed that the principal interactions were hydrogen and halogen bonding with the amino acids of Val 25 and Thr 30 in the B chain and A chain, respectively, which could be a suitable inhibitor to combat the COVID-19.

Keywords: ADMET; alkaloids; COVID-19; coronavirus; ion channel; molecular docking; molecular dynamics; SARS-CoV-2.

1. Introduction

The emergence of a new coronavirus termed severe acute respiratory syndrome coronavirus 2 (SARS-CoV-2) at the end of 2019 led to an epidemic in several Chinese provinces, including Wuhan. The World Health Organization (WHO) declared a state of crisis and gave it the official name of COVID-19 after the death toll exceeded 1,000. The latest cases and death rates in the world as of September 2021 were more than 219 and 4.55 million, respectively. The most common symptoms of this disease are fever, myalgia, dry cough, chest pain, and fatigue. Still, in some cases, dizziness, nausea, diarrhea, sore throat, rash, and paleness of the fingers and toes are observed [1], and even in rare cases, patients lose their taste and smell sense [2].

The various similarities of the virus with SARS and MERS caused epidemics in multiple nations worldwide in 2002 and 2012, respectively, placing it within the *Coronaviridae* family and *Coronavirinae* subfamily [3,4]. Cryo-electron microscopic studies have revealed that the corona is a spherical virus with approximately 125 nm diameter [5]. Coronaviruses

contain envelope and single-stranded RNA. They are divided into four different groups: alpha, beta, gamma and, delta. The COVID-19 is considered the Betacoronavirus [6]. The virus has four main structures: nucleocapsid, membrane, spike, envelope, and several non-structural proteins [7]. In this way, each protein plays a vital role in the virus's life and reproduction.

The E protein with an 8-12 kDa weight has an ion channel activity with two different terminals, including an N-terminal ectodomain and a C-terminal endodomain, as shown in Figure 1 [8-10]. Protein E is surrounded by protein M and consists of 75 to 109 amino acids and an α-helical transmembrane. The role and function of the E protein (viroporin ion channel) have not been clarified completely, but it is expected to regulate ionic balance inside and outside the cell, which is very critical in the life and pathogenesis of the virus. However, others have recommended that E protein may promote viral release by modifying the host secretory pathway [11]. It has been reported that the protein has a pathogenic function in the SARS and MERS viruses. Stated that mice infected with the coronavirus lacking the E protein reduced mortality [12]. Viruses such as hepatitis C, HIV-1, and influenza A that cause human disease are RNA viruses that express viroporin [13].

Nowadays, the expansion of complementary therapies, natural medication are finding their place. Fallah *et al.* (2021) [14] stated that natural compounds in the essential oil and extract belonging to *Panax ginseng* and *Sambucus nigra* demonstrate a potential affinity against the SARS-CoV-2 spike RBD. Alkaloids with bioactive characteristics are notable compounds in pharmaceutical industries [15]. Alkaloid compounds such as atropine, capsaicin, colchicine, and trigonelline had antiviral impacts on RNA and DNA of HSV-1 and PI-3 viruses, respectively [16]. Alkaloids are known for representing a broad spectrum of biological characteristics, such as being Ca^{+2} channel blockers and enzyme inhibitors [17], being antimalarial [18], cytotoxic [19], anti-infective, and antimicrobial [20]. Previous research reported that alkaloids such as isoboldine have a significant inhibitory effect on SARS-COV-2 protease and showed excellent oral absorption [21]. Polycyclic guanidine alkaloids isolated from *Monanchora* n. sp. were examined for antiviral potentials against five COVID-19 proteins (nsp10, main protease, membrane glycoprotein, spike glycoproteins, and nucleocapsid phosphoprotein), compounds of Crambescidin 786 and Crambescidin 826 exhibited promising *in silico* ADMET, and the best binding modes and free energies results [22]. Another study reported that quinoline and quinazoline Alkaloids such as norquinadoline A, deoxynortryptoquivaline, and deoxytryptoquivaline inhibited three protein targets of SARS-COV-2 and showed excellent pharmacokinetic and safety profiles [23].

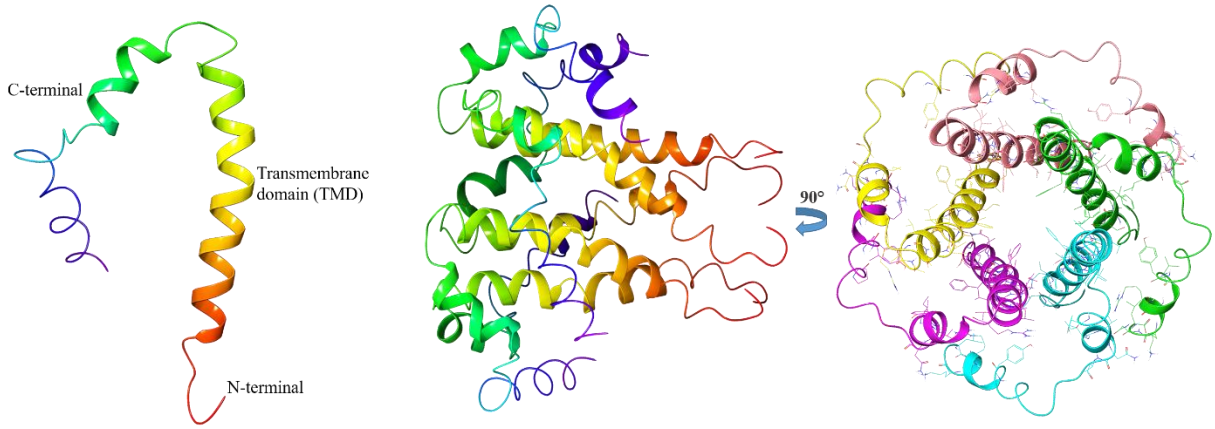

Figure 1. Pentameric ion channel of SARS CoV-2 (PDB: 5X29).

Particular medication or vaccine production process requires at least ten years from bench research to approve [24,25]. At the moment, performing computational design and drug discovery can considerably reduce both the cost and the time required for medication development [26]. In addition, the successive mutations of the COVID-19 and the lack of definitive treatment, this study aims to find a suitable and potent inhibitor using molecular docking and dynamics simulation to prevent replication of the virus. The interaction of the hit compounds with the E protein will be examined; it shows how the receptor is blocked and disturb the internal balance of the virus. On the other hand, it will show the ADMET properties of hit poses.

2. Materials and Methods

2.1. Preparation of alkaloid structures.

More than 3200 natural alkaloid compounds were obtained from Database for Rapid Dereplication of Known Natural Products (DEREP-NP) openly obtainable at (https://github.com/clzani/DEREP-NP) then prepared through LigPrep software of maestro Schrödinger 2015. To create the required 3D structures, the ionization state and compounds' chirality of the compounds remained intact, the present salts were removed, and only one structure holding the minimum energy was generated for each alkaloid compound.

2.2. Preparation of receptor.

The NMR structure of the pentameric ion channel of the coronavirus was obtained from the protein data bank (PDB ID: 5X29, https://www.rcsb.org). Optimization of the receptor was performed using the Protein preparation program of the maestro Schrödinger package 10.5 (2015). In the preparation process, hydrogen atoms were added to the amino acids, zero-order metal bonds and disulfide bonds were formed in the protein's chains. Missing loops and side chains were created by Prime software. Selenomethionine was converted to methionine, and water molecules were removed beyond 3 Å from the het groups. The PROPKA was employed to predict the pKa of ionizable groups of the receptor at pH 7.00. Ultimately, the OPLS3 force field optimized and minimized the pentameric ion channel of SARS-CoV-2.

2.3. Active binding site identification.

Active site prediction is required for molecular docking in a suitable position. According to Abreu *et al.* (2020) [27], establishing the hydrogen bonds with amino acid residues of Phe 26 and Ala 22 blocks the channel. The Sitemapping application was used for the prediction and validation of the active site (Maestro 10.5). For this purpose, the site map with a site score of more than one was selected as an active pocket site among five predicted sites. According to the mentioned information, the grid box was made in midpoints (X: -0.35, Y: -0.01, Z: -0.22) and with suitable dimensions (X, Y, Z: 20 Å) by Receptor Grid Generation Schrödinger package.

2.4. Molecular docking study.

The glide of maestro Schrödinger was used to dock alkaloid compounds and investigate their interaction with amino acid residues in the active binding site of the E protein (5X29). A partial charge of 0.15, as well as a scaling factor of 0.8, was used to soften the potential for

nonpolar parts of the compounds. In the docking process, entire compounds were considered flexible and rotated freely (nitrogen inversions and ring conformations). First of all, a large number of the ligands were docked with high throughput virtual screening (HTVS) precision for fast virtual screening and identifying effective alkaloids, then 30% of the best poses with the highest docking scores were examined for XP (extra precision) docking. Finally, more than 200 hit compounds were selected for further analysis. Molecular docking results were expressed in kcal/mol.

2.5. Free binding energy.

Prime molecular mechanics generalized Born surface area (MM-GBSA) module was applied to calculate the sum of entire intermolecular interactions in the protein-ligand complex. The free energy calculation was performed for the complex according to the MM-GBSA method and the following equation. However, other methods are also used, including free energy perturbation as well as molecular mechanics Poisson-Boltzmann surface area (MM-PBSA) [28]. The solvation model and force field in this process were considered VSGB 2.0 and OPLS3e, respectively.

$$\Delta G_{bind} = G_{complex} - (G_{ligand} + G_{receptor})$$

2.6. ADMET prediction.

The pharmacokinetic properties of the alkaloid compounds were investigated using QikPrep software. Drug-like characteristics such as molecular weight (MW), H-bond donor, H-bond acceptor, central nervous system (CNS), logPo/w, polar surface area (PSA), PCaco, brain/blood partition coefficient (logBB), percentage of oral absorption, and metabolism, which are one of the most significant steps in drug discovery, were evaluated for hit compounds.

2.7. Molecular dynamics simulation.

Molecular dynamics simulation for top-scoring alkaloid compound complexed with COVID-19 E protein studied through Macro Model software from Schrödinger maestro suite (2020). The stochastic dynamics procedure was used because it includes random forces that simulate the buffering of a system by solvent molecules. Ligand energy in an aqueous solvent and extended cutoff was minimized using the OPLS3e force field. Polak-Ribier Conjugate Gradient (PRCG) method restarts every 3N iterations at a maximum iteration of 2500 and a convergence threshold of 0.05 for complex minimization. Eventually, simulation was provided using the stochastic dynamics procedure at a simulation temperature of 300 K, a time step of 1.5 fs, and an equilibration time of 1 ps. Finally, 100 ps was considered for simulation time.

3. Results and Discussion

The development of new antiviral drugs is a time-consuming process that requires complex clinical trials. Molecular docking is a new approach that requires less time and cost in screening millions of molecules. Also, it can be a powerful tool against disease [29]. The interactions and inhibitory effects of natural alkaloids on the coronavirus ion channel were studied by molecular docking. The molecular docking of 3,200 alkaloids resulted in the selection of 25 compounds (Figure 2), which all had a docking score of less than -8.09 kcal/mol.

The free binding energy calculation and pharmacokinetic characteristics were employed to achieve these 25 alkaloid compounds. Psammaplysin U (NA-1) with the lowest docking score (-13.26 kcal/mol) and the lowest glide emodel (-67.93 kcal/mol) was determined to have the best interaction with the protein. The lowest free binding energy (ΔG_{bind}) of -93.11 kcal/mol was obtained for the purpurealidin D compound as the most stable hit pose. The docking score, free binding energy, and natural alkaloids interactions with E protein are described in Table 1.

Table 1. Docking and free binding energy scores (kcal/mol), with involved amino acids in interaction.

No.	Molecule Name	docking score	glide emodel	ΔG_{Bind}	Amino acid Interaction
NA-1	Psammaplysin U	-13.258	-93.673	-87.757	Thr 30, Val 29, Val 25, Leu 28
NA-2	Nocobactin NA	-11.322	-78.634	-85.722	Arg 61
NA-3	Purpurealidin D	-11.268	-90.744	-93.015	Thr 30
NA-4	Pyrinodemin A	-11.016	-72.815	-82.528	Phe 26
NA-5	Psammaplysin S	-10.788	-84.019	-77.567	Arg 61, Thr 30
NA-6	Araplysillin V	-10.522	-69.969	-60.201	Thr 30
NA-7	19-hydroxypsammaplysin W	-9.848	-72.915	-76.823	Leu 28
NA-8	Psammaplysin V	-9.800	-82.253	-91.450	Thr 30, Leu 28
NA-9	4-Phenylbutyl glucosinolate	-9.729	-55.042	-51.369	Ala 22, Leu 18, Asn 15, Phe 26
NA-10	N-desmethylthaxtomin C	-9.637	-41.113	-34.061	Ala 22, Phe 23
NA-11	Psammaplysin W	-9.534	-77.171	-82.854	Thr 30, Phe 26
NA-12	Montamine	-9.430	-79.448	-68.230	Thr 30, Phe 26
NA-13	Araplysillin IV	-9.374	-70.125	-64.808	Thr 30
NA-14	Gluconasturtiin	-9.080	-48.692	-47.454	Ile 46, Arg 61, Phe 26
NA-15	19-hydroxypsammaplysin T	-8.882	-79.716	-78.062	Arg 61
NA-16	2,4-Dinitrophenylhydrazone-1,7-Diphenyl-4,6-heptadien-3-one	-8.770	-58.193	-66.666	Phe 26
NA-17	Antibiotic L 654040	-8.641	-65.389	-44.457	Phe 26, Leu18, Asn15
NA-18	Dehydroascorbic acid-2,3-Bisphenylhydrazone	-8.569	-44.134	-53.469	Thr 30, Phe 26
NA-19	Psammaplysin P	-8.506	-84.687	-89.222	Thr 30, Arg 61
NA-20	O1-[3-(methyl-[1,3,4]oxadiazol-2-yl)-phenyl]-beta-D-glucopyranuronic acid	-8.419	-50.621	-54.133	Ile 46, Asn 64
NA-21	Pyrinodemin B	-8.415	-68.287	-75.003	Phe 26
NA-22	Araplysillin VI	-8.245	-82.991	-74.214	Thr 30, Arg 61
NA-23	7-Chlor-2-ethylamino-5-phenyl-3H-1,3,4-benzotriazepin	-8.148	-39.451	-46.747	Phe 26, Phe 23
NA-24	Aurachin A	-8.144	-44.934	-62.567	Arg 61
NA-25	2-Amino-7-chlor-5-phenyl-1,3,4-benzotriazepin	-8.091	-34.291	-40.995	Phe 26, Phe 23

3.1. Interactions of top-scoring alkaloid compounds with pentameric ionic channel.

The top six compounds with the highest docking score (-13.258 to -10.522 kcal/mol) are psammaplysin U, nocobactin NA, purpurealidin D, Pyrinodemin A, Psammaplysin S, and Araplysillin V, respectively. 2D and 3D interactions between the pentameric ion channel and the hit poses are shown in Figures 3-8. Compound NA-1, which has halogen and H-bond interactions with Thr 30, Val 29, Val 25, and Leu 28 amino acids, possesses the highest binding affinity of -13.258 kcal/mol with E protein pentameric ion channel (5X29). Furthermore, the free binding energy of -87.75 kcal/mol of psammaplysin U indicates the stability of the compound at the binding site. Carbonyl oxygen with Thr 30 amino acid in the chain A, the nitrogen atoms of the amide with Val 25, and hydroxyl with Val 29 in chain B form a hydrogen bond, while Leu 28 in B chain form a halogen bond with the bromine of benzene ring (Figure 3). Biological activities such as antimalarial, anti-HIV, antifouling, and cytotoxic activity were demonstrated by psammaplysin derivatives extracted from nine different species of Verongida sponge [30-32]. The NA-1 compound contains an isobranch monoenoeic fatty acid with the

molecular formula of $C_{38}H_{53}Br_4N_3O_7$, which can be extracted from the Balinese marine sponge (*Aplysinella strongylata*). Nocobactin NA (NA-2) interacts with the amino acid of Arg 61 in the E chain. The hydroxyl and the oxygen atom of the carbonyl group of NA-2 establish hydrogen bonds with the amino acid simultaneously.

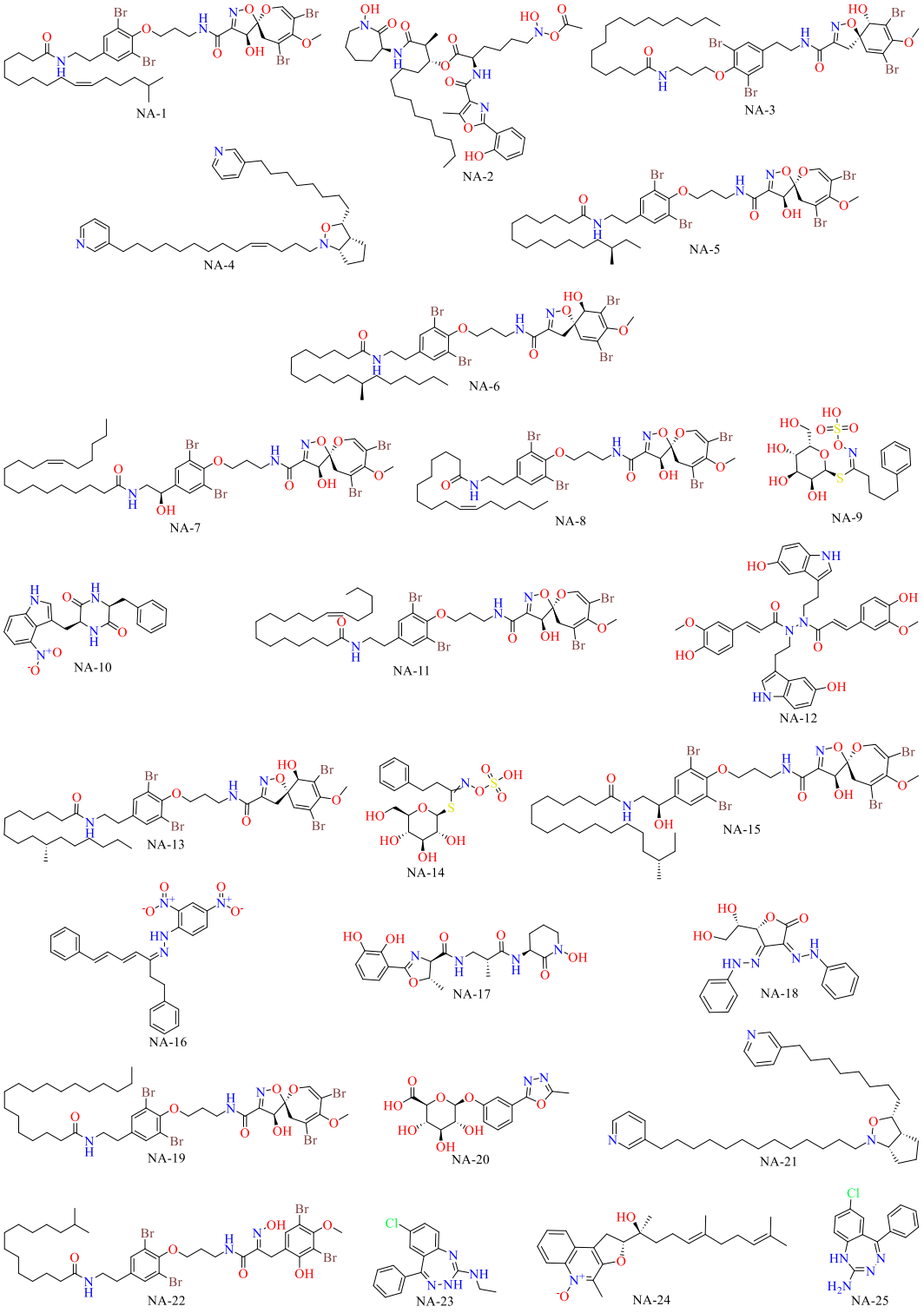

Figure 2. The 2D chemical structure of top-scoring alkaloids.

Also, a docking score of -11.32 kcal/mol and free binding energy of -85.72 kcal/mol was calculated for the compound (Figure 4). Nocobactin NA is produced by *Nocardia asteroid* and *Nocardia farcinica*, which usually grow before iron. NA-2 is a lipid-soluble compound

whose tumor-specific cytotoxicity properties were shown by Sakagami *et al.* (2005) [33]. The oxygen of the carboxyl and carbonyl group in the compound of Purpurealidin D leads to a binding affinity of -11.28 kcal/mol by forming hydrogen bonds with the amino acid of Thr 30 in chain A. The desired compound with a free energy of -93.01 kcal/mol in the pentameric ion channel was selected as the third effective compound in this study (Figure 5). The purpurealidin D is a compound of Bromotyrosine alkaloids found in sponge *Psammaplysilla purpurea* [34].

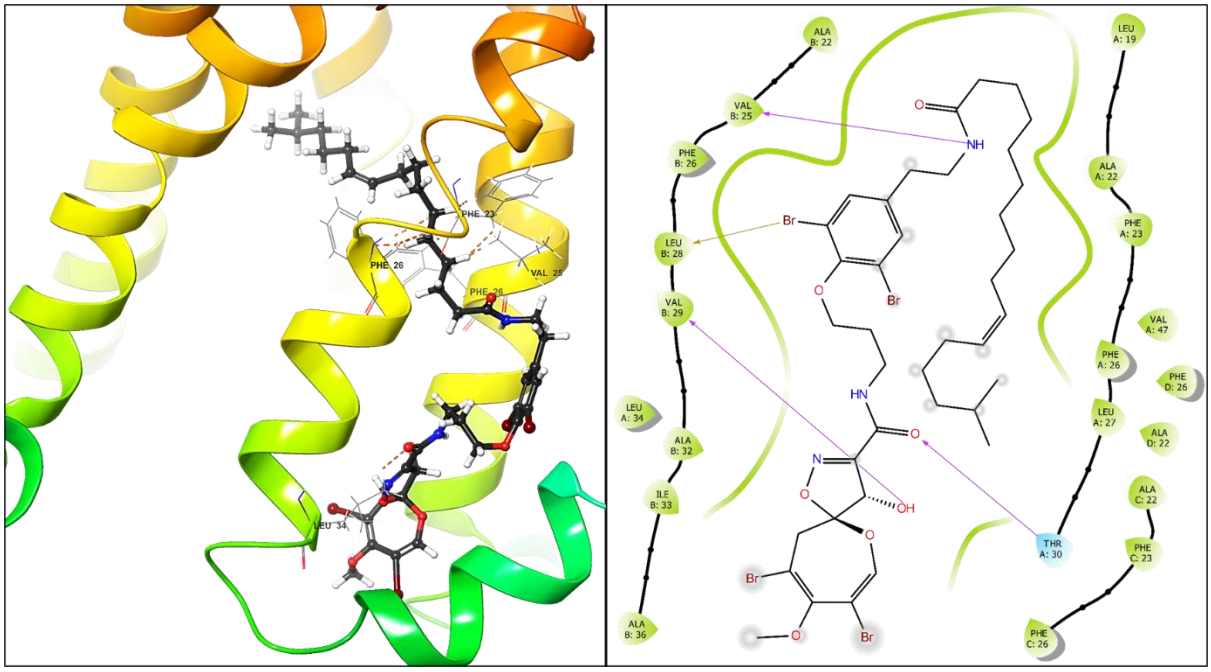

Figure 3. The 2D and 3D interaction of the pentameric ion channel - Psammaplysin U complex. The 2D map shows the importance of the involved amino acid in the binding site.

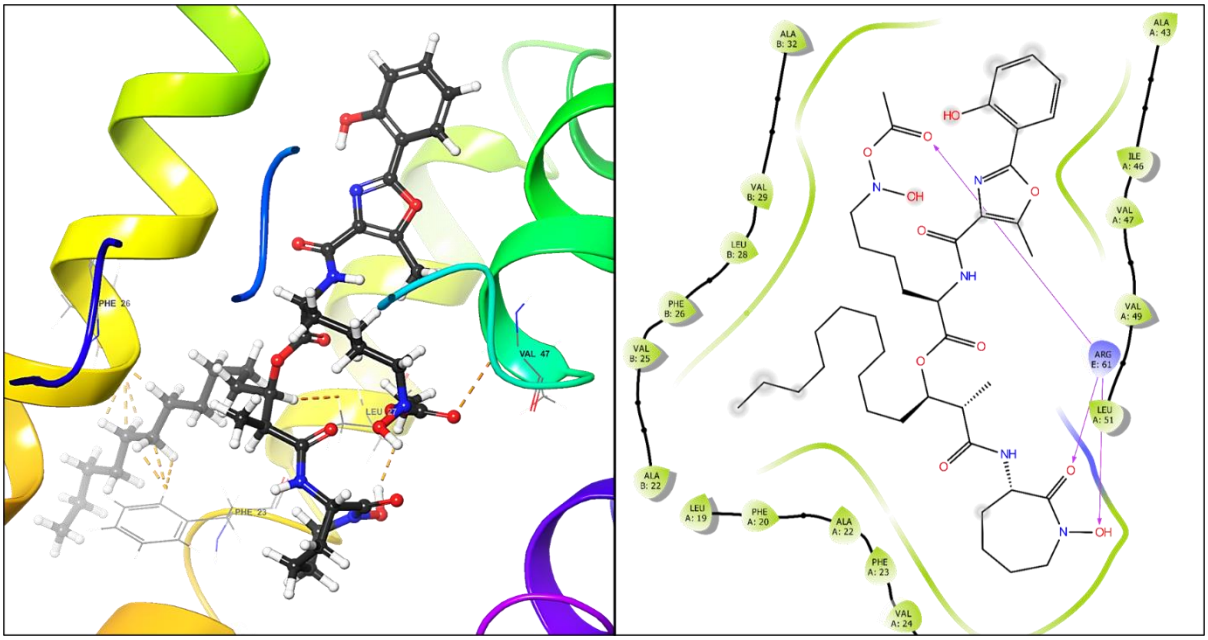

Figure 4. The 2D and 3D interaction of the pentameric ion channel - Nocobactin NA complex. The 2D map shows the importance of the involved amino acid in the binding site.

The free binding energy of Pyrinodemin A was calculated as -82.53 kcal/mol, and the docking score energy was estimated at -11.02 kcal/mol. In Figure 6, it can be seen that the pyridine ring in the NA-4 compound induces a π-π stacking with Phe 26 in the C chain, which blocks the ionic channel and disturbs the internal balance of the virus. Pyrinodemin A, with the

molecular formula of $C_{38}H_{59}N_3O$, is a cytotoxic pyridine alkaloid found in Kinawan marine sponge (*Amphimedon sp.*). Tesuda *et al.* (1999) [35] reported that the NA-4 compound had cytotoxic properties against murine leukemia with IC_{50} = 0.058 µg/ml.

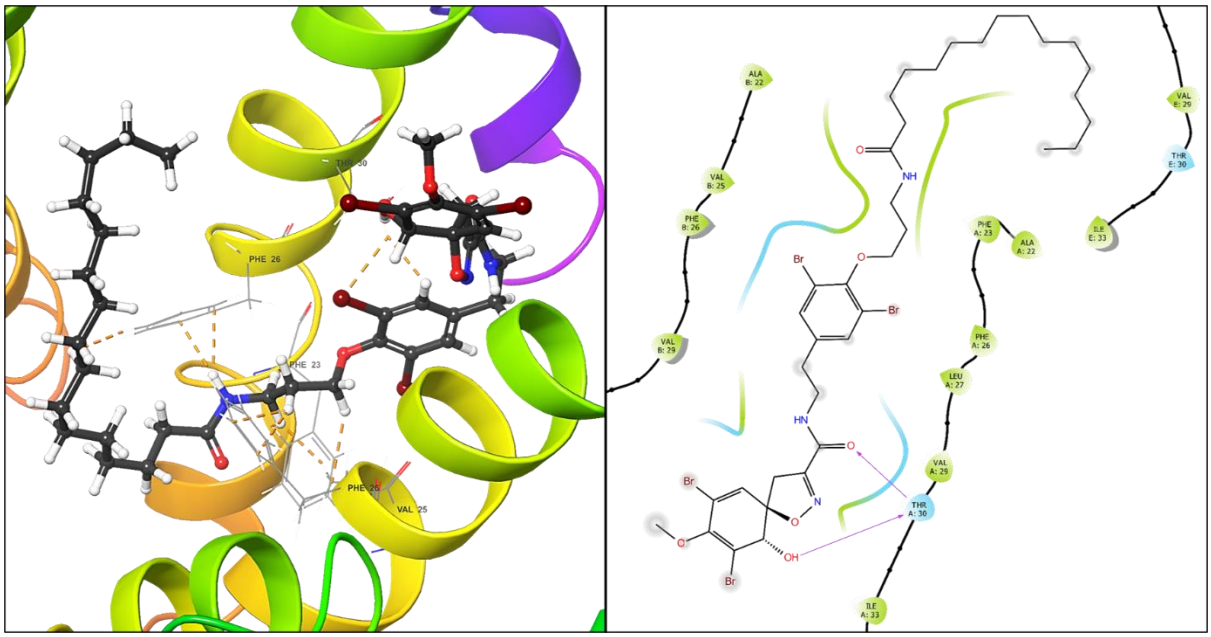

Figure 5. The 2D and 3D interaction of the pentameric ion channel - Purpurealidin D complex. The 2D map shows the importance of the involved amino acid in the binding site.

This compound has antiviral characteristics due to isoxazolidine scaffolds. NA-5 compound (Psammaplysin S) exhibits docking energy of -10.79 kcal/mol and free energy of -84.01 kcal/mol by forming hydrogen interactions with protein E. The nitrogen of the isoxazole ring creates an H-bond with the amino acid of Arg 61 in chain D. Moreover, the Thr 30 in chain E forms a hydrogen bond with the amide group's nitrogen atom (Figure 7).

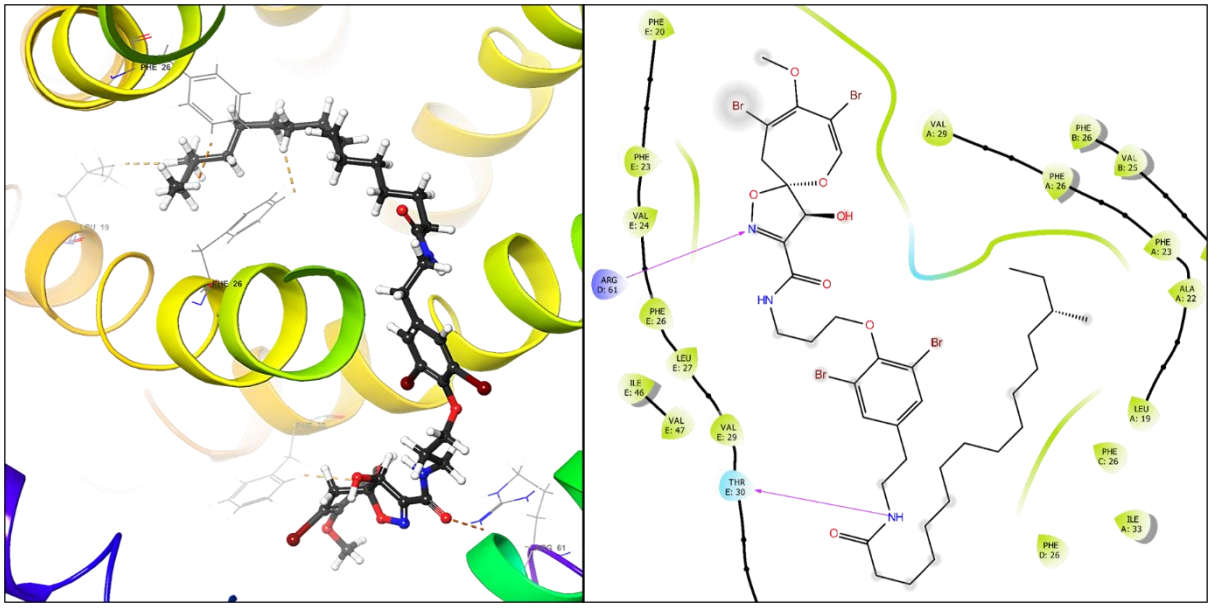

Figure 6. The 2D and 3D interaction of the pentameric ion channel - Pyrinodemin A complex. The 2D map shows the importance of the involved amino acid in the binding site.

Figure 8 shows the hydrogen bond interaction of the Araplysillin V (NA-6) compound with Thr 30 in the A chain, resulting in a binding affinity of -10.53 kcal/mol and free energy

of -60.20 kcal/mol. *Suberea ianthelliformis* sponge contains Araplysillin V, which has an antiplasmodial effect with IC_{50} = 50.5 µM [36].

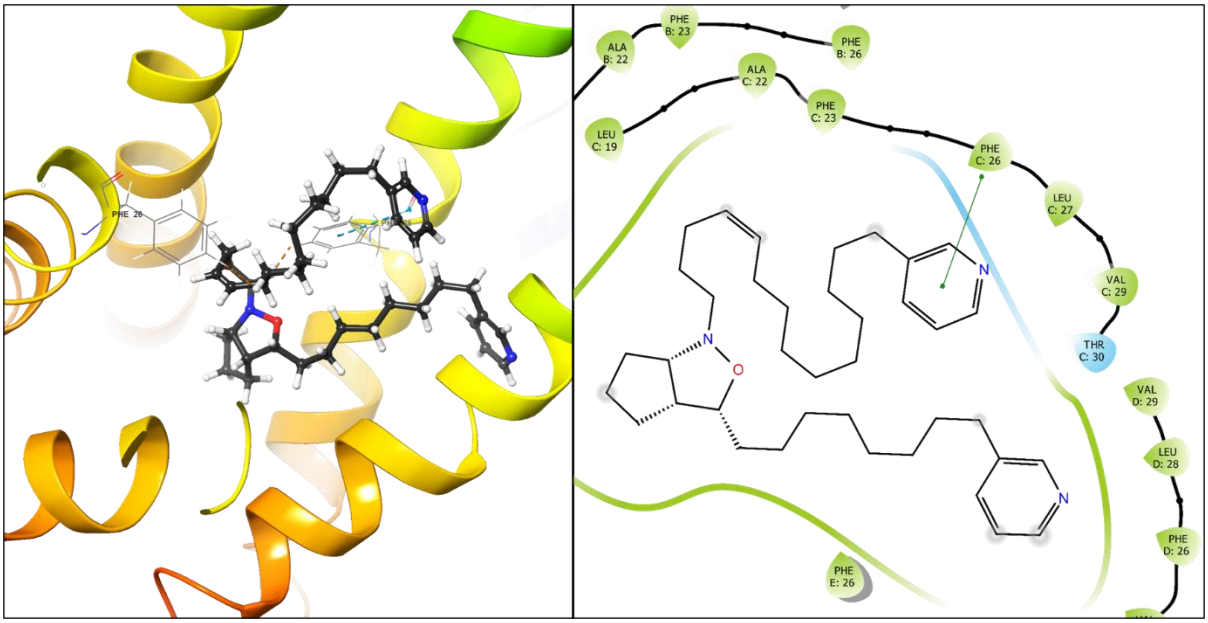

Figure 7. The 2D and 3D interaction of the pentameric ion channel - Psammaplysin S complex. The 2D map shows the importance of the involved amino acid in the binding site.

3.2. ADMET prediction.

Drug-likeness properties for alkaloid compounds were calculated by the QikProp panel and filtered the compounds to the 25 final hit poses. Lipinski's rule of 5 (molecular weight, octanol-water partition coefficient, hydrogen acceptor and donor), toxicity-related descriptors (PCaco, logBB, percentage of oral absorption, and CNS activity), and several parameters, including metabolism and PSA (Veber rule), were predicted. According to the results in Table 2, these natural alkaloid compounds proved agreeable *in silico* pharmacokinetic properties. One of the most prominent features of the drug is absorption, which makes it easy to use.

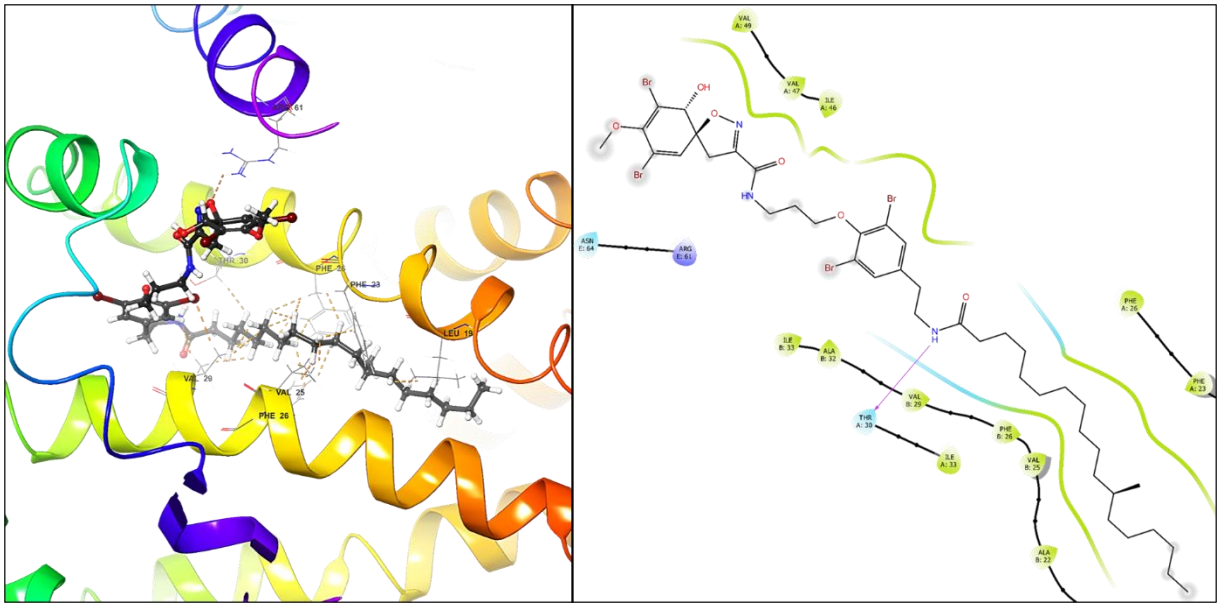

Figure 8. The 2D and 3D interaction of the pentameric ion channel - Araplysillin V complex. The 2D map shows the importance of the involved amino acid in the binding site.

The factor of log P indicates the hydrophilicity of the drug, which the high value of the log P leads to a decrease in drug absorption. All hit alkaloids except compounds of NA-9, NA-12, NA-14, NA-17, and NA-20 had an oral absorption of more than 50%. Among the top 6 selected compounds, NA-1, NA-4, NA-5, and NA-6 showed 100% oral absorption, and NA-3 compounds noted more than 95% absorption. CNS activity of the entire 25 compounds except for NA-4, NA-23, NA-24, and NA-25 were reported -2. However, the compounds mentioned were in an acceptable range with no penetration into the central nervous system. Besides, hydrogen acceptors and donors displayed great results for all 25 alkaloids. Additional information on ADMET properties is presented in Table 2.

Table 2. Pharmacokinetic properties of natural alkaloids.

No.	MW	PSA	H-Do	H-Ac	CNS	Absorption (%)	PCaco	Log BB	Log P	Metab
NA-1	983.469	135.784	2	9.7	-2	100	344.159	-2.259	9.923	7
NA-2	787.949	245.202	2.5	14.95	-2	52.587	37.675	-4.539	6.201	6
NA-3	955.458	133.900	3	9.95	-2	95.317	148.431	-2.983	9.465	6
NA-4	573.904	36.087	0	6.2	-2	100	735.423	-1.053	8.996	8
NA-5	985.484	139.250	2	9.7	-2	100	258.206	-2.629	10.177	5
NA-6	997.539	134.553	3	9.95	-2	100	151.544	-3.040	10.147	6
NA-7	1027.522	155.531	3	11.4	-2	86.212	184.076	-3.180	9.838	7
NA-8	969.442	143.883	2	9.7	-2	100	179.631	-2.711	9.750	7
NA-9	451.506	186.037	5	14	-2	33.827	2.407	-3.639	0.009	7
NA-10	378.387	134.819	3	6	-2	57.631	21.631	-1.986	1.160	5
NA-11	1011.522	139.583	2	9.7	-2	100	233.745	-2.705	10.365	7
NA-12	702.762	179.344	6	9.5	-2	26.561	11.254	-4.447	5.573	8
NA-13	969.485	131.902	3	9.95	-2	100	200.475	-2.761	9.819	6
NA-14	423.452	173.035	5	14	-2	39.845	6.672	-2.890	-0.317	7
NA-15	1029.537	160.514	3	11.4	-2	83.444	114.779	-3.581	9.992	5
NA-16	442.473	108.481	1	4	-2	88.788	172.307	-2.390	5.939	5
NA-17	434.448	179.740	3.25	11.45	-2	36.794	21.226	-2.607	-0.161	5
NA-18	354.365	121.243	3	9.4	-2	81.276	318.413	-1.689	1.628	7
NA-19	999.511	132.931	2	9.7	-2	100	383.693	-2.585	10.518	5
NA-20	352.300	168.502	3	11.05	-2	39.395	5.366	-2.588	-0.104	6
NA-21	561.893	41.365	0	6.2	0	100	907.398	-0.978	9.096	6
NA-22	941.431	141.081	3	8.95	-2	95.255	132.032	-3.136	9.610	6
NA-23	298.774	62.154	2	3.5	1	100	2230.237	0.010	3.821	0
NA-24	395.541	46.688	1	2.5	0	100	2860.122	-0.546	6.888	10
NA-25	270.721	78.453	3	3.5	-1	89.643	531.048	-0.483	2.378	0

MW = Molecular weight (g/mol); PSA = Polar surface area; H-Ac = No. of hydrogen bond acceptors; H-Do = No. of hydrogen bond donors; CNS = Central nervous system; Absorption (%) = Percentage of human oral absorption; PCaco = Predicted Caco-2 cell permeability; LogBB = brain/blood partition coefficient; LogP = Predicted octanol/water partition coefficient; Metab = Metabolism

3.3. Molecular dynamics analysis.

Molecular dynamics simulation was used to understand the bonds in the ligand-ion channel complex accurately. Molecular dynamics simulations were evaluated for a 100 ps trajectory to achieve the top ligand's stability and mechanism of interaction with the pentameric ion channel in 150 frames. The system hit a stable equilibrium after about 60 picoseconds from the simulation process (Figure 9).

According to the standard, the convergence threshold was considered 0.05, and if a difference of 0.05 kJ/mol is observed between at least two calculated potential energies, the system will iteratively be optimized. The simulation's film shows that the first interaction of ligand-protein is the nitrogen atom of Psammaplysin U with the Val 25 in the B chain. Besides, in the equilibrium times, the most interactions were the halogen bond of the bromine with Thr 30 in chain A.

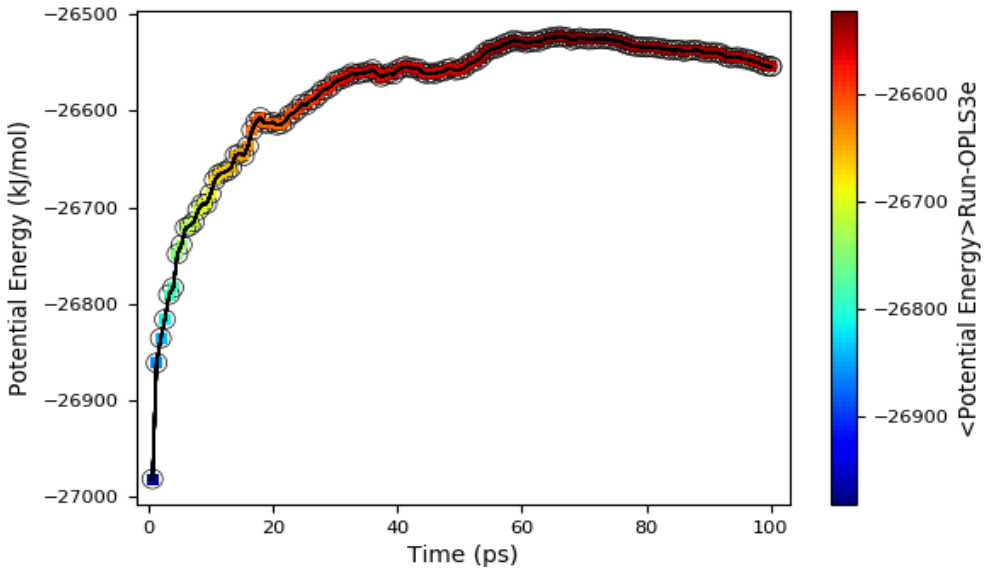

Figure 9. Convergence graph of the pentameric ion channel-Psammaplysin U complex in terms of potential energy.

4. Conclusions

The present study was performed to identify and determine an appropriate inhibitor of natural alkaloid compounds to block the ion channel of the coronavirus in the current situation with no definite medication. The compounds of NA-1 to NA-6 with the highest docking score were identified as hit poses by molecular docking study. Post-screening analyses such as free binding energy and pharmacokinetic characteristics have not been ineffective in selecting these compounds. So that among these compounds, the most stable compound in the presence of protein is NA-3 with -93.01 kcal/mol, and the unstable compound with the energy of -60.20 kcal/mol was NA-6. Finally, the compound of Psammaplysin U with docking score of -13.26 kcal/mol, glide emodel of -93.67 kcal/mol, and hydrogen interactions with amino acids of Val 25, and Val 29 in the chain B, Thr 30 in chain A, also halogen interaction with Leu 28, was selected as the superior alkaloid compound. The first interaction in the molecular dynamics simulation was the hydrogen bond of the NA-1 compound with the amino acid of Val 25 in the B chain of the virus's ion channel. Psammaplysin U could be a suitable compound for equilibrium disruption of the virus and ultimately the disease therapy.

Funding

This research received no external funding.

Acknowledgments

The authors thank the Research Council of Shahid Beheshti University, Tehran, Iran, for their financial support.

Conflicts of Interest

The authors declare no conflict of interest.

References

1. Harapan, H.; Itoh, N.; Yufika, A.; Winardi, W.; Keam, S.; Te, H.; Megawati, D.; Hayati, Z.; Wagner, A.L.; Mudatsir, M. Coronavirus disease 2019 (COVID-19): A literature review. *Journal of infection and public health* **2020**, https://doi.org/10.1016/j.jiph.2020.03.019.
2. Marshall, M. COVID's toll on smell and taste: what scientists do and don't know. *Nature* **2021**, https://doi.org/10.1038/d41586-021-00055-6.
3. Fehr, A.R.; Perlman, S. Coronaviruses: an overview of their replication and pathogenesis. *Coronaviruses* **2015**, https://doi.org/10.1007/978-1-4939-2438-7_1.
4. Sumirtanurdin, R.; Barliana, M.I. Coronavirus disease 2019 vaccine development: an overview. *Viral Immunology* **2021**, *34*, 134-144, https://doi.org/10.1089/vim.2020.0119.
5. Neuman, B.W.; Adair, B.D.; Yoshioka, C.; Quispe, J.D.; Orca, G.; Kuhn, P.; Milligan, R.A.; Yeager, M.; Buchmeier, M.J. Supramolecular architecture of severe acute respiratory syndrome coronavirus revealed by electron cryomicroscopy. *Journal of virology* **2006**, *80*, 7918-7928, https://doi.org/10.1128/JVI.00645-06.
6. Lu, R.; Zhao, X.; Li, J.; Niu, P.; Yang, B.; Wu, H.; Wang, W.; Song, H.; Huang, B.; Zhu, N. Genomic characterisation and epidemiology of 2019 novel coronavirus: implications for virus origins and receptor binding. *The lancet* **2020**, *395*, 565-574, https://doi.org/10.1016/S0140-6736(20)30251-8.
7. Troyano-Hernáez, P.; Reinosa, R.; Holguín, Á. Evolution of SARS-CoV-2 Envelope, Membrane, Nucleocapsid, and Spike Structural Proteins from the Beginning of the Pandemic to September 2020: A Global and Regional Approach by Epidemiological Week. *Viruses* **2021**, *13*, 243, https://doi.org/10.3390/v13020243.
8. DeDiego, M.L.; Álvarez, E.; Almazán, F.; Rejas, M.T.; Lamirande, E.; Roberts, A.; Shieh, W.-J.; Zaki, S.R.; Subbarao, K.; Enjuanes, L. A severe acute respiratory syndrome coronavirus that lacks the E gene is attenuated in vitro and in vivo. *Journal of virology* **2007**, *81*, 1701-1713, https://doi.org/10.1128/JVI.01467-06.
9. Godet, M.; L'Haridon, R.; Vautherot, J.-F.; Laude, H. TGEV corona virus ORF4 encodes a membrane protein that is incorporated into virions. *Virology* **1992**, *188*, 666-675, https://doi.org/10.1016/0042-6822(92)90521-P.
10. Hasan, S.; Hossain, M.M. Analysis of COVID-19 M protein for possible clues regarding virion stability, longevity and spreading. **2020**, https://doi.org/10.31219/osf.io/e7jkc.
11. Buzon, M.J.; Seiss, K.; Weiss, R.; Brass, A.L.; Rosenberg, E.S.; Pereyra, F.; Xu, G.Y.; Lichterfeld, M. Inhibition of HIV-1 integration in ex vivo-infected CD4 T cells from elite controllers. *Journal of virology* **2011**, *85*, 9646-9650, https://doi.org/10.1128/JVI.05327-11.
12. Jimenez-Guardeño, J.M.; Nieto-Torres, J.L.; DeDiego, M.L.; Regla-Nava, J.A.; Fernandez-Delgado, R.; Castaño-Rodriguez, C.; Enjuanes, L. The PDZ-binding motif of severe acute respiratory syndrome coronavirus envelope protein is a determinant of viral pathogenesis. *PLoS Pathog* **2014**, *10*, e1004320, https://doi.org/10.1371/journal.ppat.1004320.
13. Madan, V.; Castelló, A.; Carrasco, L. Viroporins from RNA viruses induce caspase-dependent apoptosis. *Cellular microbiology* **2008**, *10*, 437-451, https://doi.org/10.1111/j.1462-5822.2007.01057.x.
14. Fallah, M.S.; Bayati, M.; Najafi, A.; Behmard, E.; Javad, S. Molecular Docking Investigation of Antiviral Herbal Compounds as Potential Inhibitors of SARS-CoV-2 Spike Receptor. *Biointerface Res. Appl. Chem* **2021**, *11*, 12916-12924, https://doi.org/10.33263/BRIAC115.1291612924.
15. Mukherjee, A.K.; Basu, S.; Sarkar, N.; Ghosh, A.C. Advances in cancer therapy with plant based natural products. *Current medicinal chemistry* **2001**, *8*, 1467-1486, https://doi.org/10.2174/0929867013372094.
16. Özçelik, B.; Kartal, M.; Orhan, I. Cytotoxicity, antiviral and antimicrobial activities of alkaloids, flavonoids, and phenolic acids. *Pharmaceutical biology* **2011**, *49*, 396-402, https://doi.org/10.3109/13880209.2010.519390.
17. Suna, H.; Aoki, S.; Setiawan, A.; Kobayashi, M. Crambescidin 800, a pentacyclic guanidine alkaloid, protects a mouse hippocampal cell line against glutamate-induced oxidative stress. *Journal of Natural Medicines* **2007**, *61*, 288-295, https://doi.org/10.1007/s11418-007-0148-5.
18. Tempone, A.G.; Pieper, P.; Borborema, S.E.; Thevenard, F.; Lago, J.H.G.; Croft, S.L.; Anderson, E.A. Marine alkaloids as bioactive agents against protozoal neglected tropical diseases and malaria. *Natural Product Reports* **2021**, https://doi.org/10.1039/D0NP00078G.
19. Shubina, L.K.; Makarieva, T.N.; von Amsberg, G.; Denisenko, V.A.; Popov, R.S.; Dyshlovoy, S.A. Monanchoxymycalin C with anticancer properties, new analogue of crambescidin 800 from the marine sponge Monanchora pulchra. *Natural product research* **2019**, *33*, 1415-1422, https://doi.org/10.1089/vim.2020.0119.
20. Youssef, F.S.; Alshammari, E.; Ashour, M.L. Bioactive alkaloids from genus Aspergillus: mechanistic interpretation of their antimicrobial and potential SARS-CoV-2 inhibitory activity using molecular modelling. *International Journal of Molecular Sciences* **2021**, *22*, 1866, https://doi.org/10.3390/ijms22041866.

21. Omrani, M.; Bayati, M.; Mehrbod, P.; Asmari Bardazard, K.; Nejad-Ebrahimi, S. Natural products as inhibitors of COVID-19 main protease–A virtual screening by molecular docking. *Pharm Sci* https://doi.org/10.34172/ps.2021.11.
22. El-Demerdash, A.; Metwaly, A.M.; Hassan, A.; El-Aziz, A.; Mohamed, T.; Elkaeed, E.B.; Eissa, I.H.; Arafa, R.K.; Stockand, J.D. Comprehensive virtual screening of the antiviral potentialities of marine polycyclic guanidine alkaloids against SARS-CoV-2 (COVID-19). *Biomolecules* **2021**, *11*, 460, https://doi.org/10.3390/biom11030460.
23. Ismail, E.M.; Shantier, S.W.; Mohammed, M.S.; Musa, H.H.; Osman, W.; Mothana, R.A. Quinoline and quinazoline alkaloids against COVID-19: an in silico multitarget approach. *Journal of Chemistry* **2021**, *2021*, https://doi.org/10.1155/2021/3613268.
24. Papaneri, A.B.; Johnson, R.F.; Wada, J.; Bollinger, L.; Jahrling, P.B.; Kuhn, J.H. Middle East respiratory syndrome: obstacles and prospects for vaccine development. *Expert review of vaccines* **2015**, *14*, 949-962, https://doi.org/10.1586/14760584.2015.1036033.
25. Thariny, E.; Girija, A.S.; Brundha, M. Challenges in the synthesis of n-CoV vaccine-A review. *Annals of the Romanian Society for Cell Biology* **2021**, 1035-1051.
26. Murphy, B.R.; Alling, D.; Snyder, M.; Walsh, E.; Prince, G.; Chanock, R.; Hemming, V.; Rodriguez, W.; Kim, H.; Graham, B. Effect of age and preexisting antibody on serum antibody response of infants and children to the F and G glycoproteins during respiratory syncytial virus infection. *Journal of clinical microbiology* **1986**, *24*, 894-898, https://doi.org/10.1128/jcm.24.5.894-898.1986.
27. Abreu, G.A.; Aguilar, M.H.; Covarrubias, D.H.; Durán, F.R. Amantadine as a drug to mitigate the effects of COVID-19. *Med Hypotheses* **2020**, *140*, 109755, https://doi.org/10.1016/j.mehy.2020.109755.
28. Ghosh, R.; Chakraborty, A.; Biswas, A.; Chowdhuri, S. Identification of alkaloids from Justicia adhatoda as potent SARS CoV-2 main protease inhibitors: An in silico perspective. *Journal of Molecular Structure* **2021**, *1229*, https://doi.org/10.1016/j.molstruc.2020.129489.
29. Meng, X.; Zhang, H.-X.; Mezei, M.; Cui, M. Molecular docking: a powerful approach for structure-based drug discovery. Curr comput-aid drug 7 (2). **2011,** 146–157, https://doi.org/10.2174/157340911795677602.
30. Copp, B.R.; Ireland, C.M.; Barrows, L.R. Psammaplysin C: a new cytotoxic dibromotyrosine-derived metabolite from the marine sponge Druinella (= Psammaplysilla) purpurea. *Journal of natural products* **1992**, *55*, 822-823, https://doi.org/10.1021/np50084a021.
31. Tsukamoto, S.; Kato, H.; Hirota, H.; Fusetani, N. Ceratinamides A and B: New antifouling dibromotyrosine derivatives from the marine sponge Pseudoceratina purpurea. *Tetrahedron* **1996**, *52*, 8181-8186, https://doi.org/10.1016/0040-4020(96)00387-0.
32. Xu, M.; Andrews, K.T.; Birrell, G.W.; Tran, T.L.; Camp, D.; Davis, R.A.; Quinn, R.J. Psammaplysin H, a new antimalarial bromotyrosine alkaloid from a marine sponge of the genus Pseudoceratina. *Bioorganic & medicinal chemistry letters* **2011**, *21*, 846-848, https://doi.org/10.1016/j.bmcl.2010.11.081.
33. Sakagami, H.; Ishihara, M.; Hoshino, Y.; Ishikawa, J.; Mikami, Y.; Fukai, T. Cytotoxicity of nocobactins NA-a, NA-b and their ferric complexes assessed by semiempirical molecular orbital method. *in vivo* **2005**, *19*, 277-282.
34. Tilvi, S.; Rodrigues, C.; Naik, C.; Parameswaran, P.; Wahidhulla, S. New bromotyrosine alkaloids from the marine sponge Psammaplysilla purpurea. *Tetrahedron* **2004**, *60*, 10207-10215, https://doi.org/10.1016/j.tet.2004.09.009.
35. Tsuda, M.; Hirano, K.; Kubota, T.; Kobayashi, J.i. Pyrinodemin A, a cytotoxic pyridine alkaloid with an isoxazolidine moiety from sponge Amphimedon sp. *Tetrahedron letters* **1999**, *40*, 4819-4820, https://doi.org/10.1016/S0040-4039(99)00852-7.
36. Mani, L.; Jullian, V.; Mourkazel, B.; Valentin, A.; Dubois, J.; Cresteil, T.; Folcher, E.; Hooper, J.N.; Erpenbeck, D.; Aalbersberg, W. New antiplasmodial bromotyrosine derivatives from Suberea ianthelliformis Lendenfeld, 1888. *Chemistry & biodiversity* **2012**, *9*, 1436-1451, https://doi.org/10.1002/cbdv.201100309.